

Novel optical neural network architecture with the temporal synthetic dimension

Bo Peng^{1,†}, Shuo Yan^{1,†}, Dali Cheng¹, Danying Yu¹, Zhanwei Liu¹,

Vladislav V. Yakovlev², Luqi Yuan^{1,*}, and Xianfeng Chen^{1,3,4,5}

¹*State Key Laboratory of Advanced Optical Communication Systems and Networks,*

School of Physics and Astronomy,

Shanghai Jiao Tong University,

Shanghai 200240, China

²*Texas A&M University,*

College Station, Texas 77843, USA

³*Shanghai Research Center for Quantum Sciences,*

Shanghai 201315, China

⁴*Jinan Institute of Quantum Technology,*

Jinan 250101, China

⁵*Collaborative Innovation Center of Light Manipulation and Applications,*

Shandong Normal University,

Jinan 250358, China

[†]*These authors contribute equally to this work.*

**Corresponding author: yuanluqi@sjtu.edu.cn*

(Dated: February 28, 2025)

Abstract

Optical neural networks, employing optical fields and photonic tools to perform artificial neural network computations, are rapidly advancing and are generating a broad interest and sparking new applications. We propose a nascent approach for realizing the optical neural network utilizing a single resonator network, where the arrival times of optical pulses are interconnected to construct a synthetic temporal dimension. The set of pulses in each roundtrip therefore provides the sites in each layer in the optical neural network, and can be linearly transformed with splitters and delay lines, including the phase modulators, when pulses circulate inside the network. Such linear transformation can be arbitrarily controlled by applied modulation phases, which serve as the building block of the neural network together with a nonlinear component for pulses. We validate the functionality of the proposed optical neural network using an example of a complicated wine classification problem. This proof of principle demonstration opens up an opportunity to develop a photonics-based machine learning in a single ring network utilizing the concept of synthetic dimensions. Our approach holds flexibility and easiness of reconfiguration with potentially complex functionality in achieving desired optical tasks, pointing towards promisingly perform on-chip optical computations with further miniaturization.

I. INTRODUCTION

Optical neural networks (ONN) have been under extensive studies recently with an ultimate goal of achieving machine learning in a photonic system, which holds a promise of providing an alternative solution to artificial intelligence compared to its more traditional realization using computers based on electrical circuits [1–10]. Recent advancements have revealed that ONN exhibits important computation capability with photonic tools [11–15] as well as training optical fields for some specific optimization purposes [16]. On the other hand, realizations of ONN on different platforms have also attracted great interest from the theoretical and computational perspectives. For example, training ONN through in situ back propagation [17, 18] and quantum ONN can conduct the non-classical tasks [19]. Nevertheless, it has been found that most of ONN designs depend on the number of photonic devices in each layer as well as the total layer number, which makes an ONN system require N^2 photonic devices with tunable externally controlled components and makes its practical implementation rather complex and lacks the freedom and options for further reconfiguration and miniaturization [11–13]. It is therefore important to find simple photonic ONN designs beyond the device size but with enough freedom towards arbitrary functionality.

Synthetic dimensions in photonics have shown to offer a novel concept of utilizing the different degrees of freedom of light [20, 21], which are found to have several practical implementations such as simplification of experimental setups [22, 23], design of the complex connectivity in synthetic dimensions [24–27], capability of further reconfigurations [28, 29], and realizations of exotic physical phenomena [30, 31]. In particular, synthetic dimensions can be achieved by using different approaches to connect optical modes with different frequencies [32–35], orbital angular momenta [36], temporal positions [37–42], and modal profiles [27]. Therefore, the concept of synthetic dimensions opens an avenue towards establishing flexible experimental platforms to explore a variety of important physics [43–46]. Most recently, it has been proposed that the ONN with the concept of synthetic dimensions provides a potential route towards the simple ONN design for complicated functionality [47–49].

In this report, we propose to achieve the optical neural network in a single resonator network, with the temporal synthetic dimension constructed by connecting different temporal positions of pulses with pairs of delay lines. The optical resonator network with reconfigurable couplings between different arrival times (i.e., temporal positions) of optical pulses

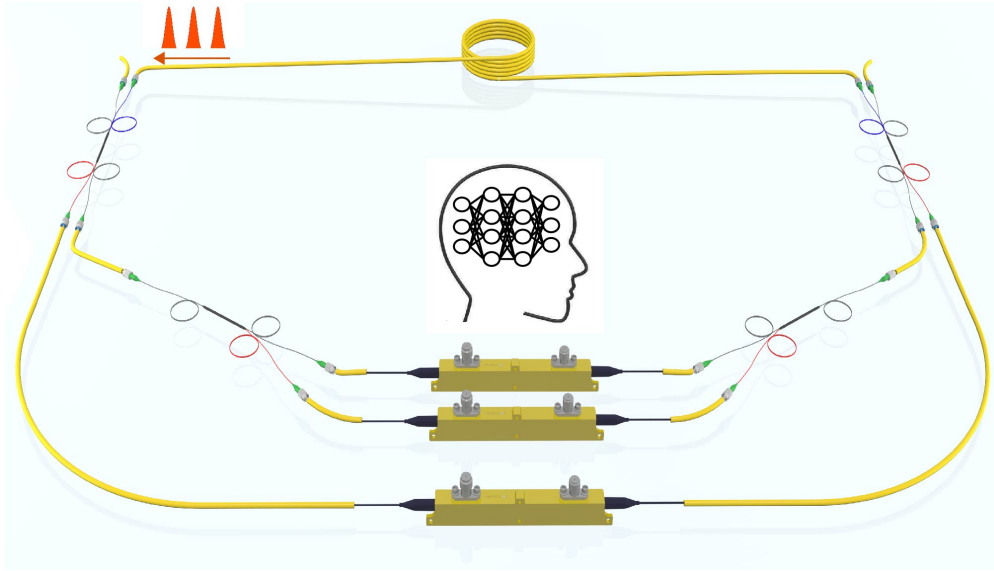


FIG. 1: Schematic of the optical neural network architecture proposed in a single ring resonator network.

supports time-multiplexed lattice [40] and creates the temporal synthetic dimension. Such system has been shown its utility in exploring many fundamental physics phenomena [40, 50]. In our present study, we consider such an optical resonator network, where splitters with modulation phases are placed at the positions connecting the main loop of the resonator and each delay line. Phase modulators are added to change phases of optical pulses that propagate through in both the main loop and delay lines. By properly controlling all modulation phases with external voltages, we show that we can construct multiple layers of ONN in a single resonator (see Fig. 1). As the validation, we perform the training of the proposed platform for ONN with the training data set of the wine classification problem [51], and our results show that such ONN with the temporal synthetic dimension exhibits the deep-learning functionality. The striking feature of our ONN is that it needs only one resonator, as compared to Ref. [47], and shows the capability of adding more connectivities between sites in two layers, which can further increase the efficiency of deep learning with a larger set of training. Our design gives arbitrary size of layers in the network, which makes our system unlimited in total layer (roundtrip) number with highly re-configurability for ONN. With the appropriate choice of the number of pulses in each roundtrip and the total number of roundtrips, this single resonator network is capable of conducting arbitrary computations with all-optical pulses, after performing the proper training. Our work hence points out

an important route towards the potential for realizing the ONN with synthetic dimensions, which is highly scalable and therefore gives the extra freedom for further simplification of the setup with possible reconfiguration.

This report is arranged as follows. We give the model of the optical neural network architecture in Section II. In Section III, we give the brief procedure of the training process in the proposed ONN. We then show the proof-of-principle example of the wine classification problem in Section IV. Afterwards, we give our conclusion.

II. MODEL

We start discussing our proposal based on the optical resonator network in Fig. 1. The resonator is composed of the main cavity loop of the waveguide [see details in Fig. 2(a)]. By neglecting the group velocity dispersion of the waveguide, we consider that there are N optical pulses in total simultaneously propagating inside the loop, and every two closet nearby pulses is temporally separated by a fixed time Δt . Each pulse can then be labelled by its temporal position t_n (or arrival time, with $t_{n+1} - t_n = \Delta t$) [40], and we can use $n = 1, \dots, N$ to denote each pulse at different temporal positions.

To construct the temporal synthetic dimension, we add a pair of delay lines, which are connected with the main cavity loop through splitters and couplers as shown in Fig. 2(a). Each splitter is controlled by a parameter $\phi_{1(2)}$, which determines that a portion of the pulse with the amplitude $\cos \phi_{1(2)}$ remains in the main loop while the rest of the pulse with the amplitude $i \sin \phi_{1(2)}$ gets into one of the delay lines [37, 38]. Lengths of both delay lines are carefully designed. For the pulse at the temporal position n propagating through the shorter delay line, it combines into the main loop at a time Δt ahead of its original arrival time t_n and contributes to the pulse at the time $t_{n-1} = t_n - \Delta t$, i.e., $\Delta n = -1$. On the other hand, for the pulse propagating through the longer delay line, it combines into the main loop at a time Δt behind its original arrival time t_n and contributes to the pulse at the time $t_{n+1} = t_n + \Delta t$, i.e., $\Delta n = +1$. Such a design constructs the temporal synthetic dimension, [see the illustration in Fig. 2(b)], where the n -th pulse during the m -th roundtrip with the amplitude $A(n, m)$ is connected to its nearest neighbor sites in the temporal synthetic lattice after each roundtrip.

In order to obtain the functionality of the ONN, we place phase modulators inside the

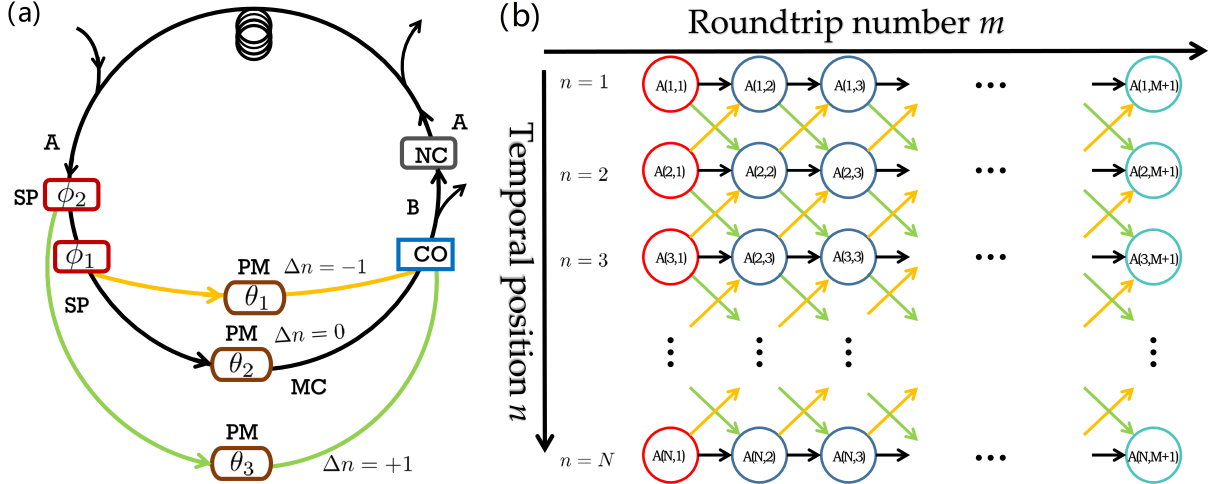


FIG. 2: (a) The schematic of the single resonator network with two delay lines in yellow and green respectively. CO: Combiner, SP: Splitter, PM: Phase modulator, NC: Nonlinear component. (b) The connectivity of the synthetic photonic lattice along the temporal dimension (n -axis) implemented in (a) for pulses evolving after roundtrips (m). A number of N pulses in each roundtrip is considered and the pulses evolve for M roundtrips in total, which therefore constructs the ONN with M layers and N neurons sites in each layer. Green, black and bright yellow arrows correspond to different optical branches of delay lines in (a).

main cavity loop as well as two delay lines. Each phase modulator is controlled by external voltage and can add a modulation phase θ_i ($i = 1, 2, 3$) for the pulse propagating through it [see Fig. 2(a)] [40]. Moreover, we add a nonlinear component, a saturable absorber, which can convert the input pulse to an output pulse with a nonlinear function [3].

Up to this point, we have introduced our schematic diagram of the single resonator network in Fig. 2, which supports the temporal synthetic dimension. One notices that parameters ϕ_i and θ_i can be precisely controlled at any time, meaning that one can manipulate ϕ_i and θ_i for each pulse n at each roundtrip number m . Input pulse(s) is injected into the single resonator network through a combiner and the output signal is collected by splitting a very small portion of the pulses out from the main cavity loop for further analysis. Hence real-time information of pulses evolution inside this network is available. In the following, we get into details of how this network with the temporal synthetic dimension can realize the ONN.

Conventional artificial neural network consists of linear transformation operation and

the nonlinear activation operation [52]. ONN architectures follow the similar procedures when light propagates through layers in the spatial dimension [3–5]. In the synthetic lattice with the connectivity along the temporal dimension in Fig. 2(b), the propagation process that the set of pulses with amplitudes $A(n, m)$ undergo beam splitters, phase modulations, and combiners in a single roundtrip can compose the linear transformation, which can be described by [37, 38]

$$\begin{aligned}
B(n, m) = & A(n, m) \cos \phi_1(n, m) \cos \phi_2(n, m) e^{i\theta_2(n, m)} \\
& - iA(n + 1, m) \sin \phi_2(n + 1, m) e^{i\theta_3(n+1, m)} \\
& - iA(n - 1, m) \cos \phi_2(n - 1, m) \sin \phi_1(n - 1, m) e^{i\theta_1(n-1, m)},
\end{aligned} \tag{1}$$

where $B(n, m)$ denotes output amplitudes for the set of pulses after the linear transformation [see Fig. 2(a)]. The pulses then pass the nonlinear component (a saturable absorber here), which can be described by [3, 53]

$$2\sigma\tau B(n, m)(1 - T_M) = \ln\left(\frac{T_M}{T_0}\right), \tag{2}$$

$$A(n, m + 1) = B(n, m)T_M, \tag{3}$$

where σ and τ denote the absorption cross-section and the lifetime of the absorber material, respectively. T_0 is the initial transmittance dependent on the absorber. For a given input pulse $B(n, m)$, the transmittance of the absorber T_M can be calculated by using Eq. (2). The output of the pulse after it passes the nonlinear component is then given by Eq. (3), which turns out to be the input pulse $A(n, m + 1)$ for the next layer (the next roundtrip).

The forward transmissions with linear transformations and nonlinear operations on pulses are performed while pulses propagate inside the single resonator network with the increase of the roundtrip number m . The combination of linear transformation and nonlinear operation in each roundtrip gives an effective layer m of the artificial neural network. Fig. 3 summarizes such forward transmission along the temporal synthetic dimension. Theoretically, the total number of layers, M as well as the total pulse number N , can be arbitrary, which determines the scalability of our proposed architecture. In Fig. 3, we use W_m to define the linear transformation in Eq. (1) and f_m to define the nonlinear operation in Eqs. (2) and (3) for the m -th roundtrip. Hence the forward transmission at each layer m can be described as:

$$B_m = W_m A_m, \tag{4}$$

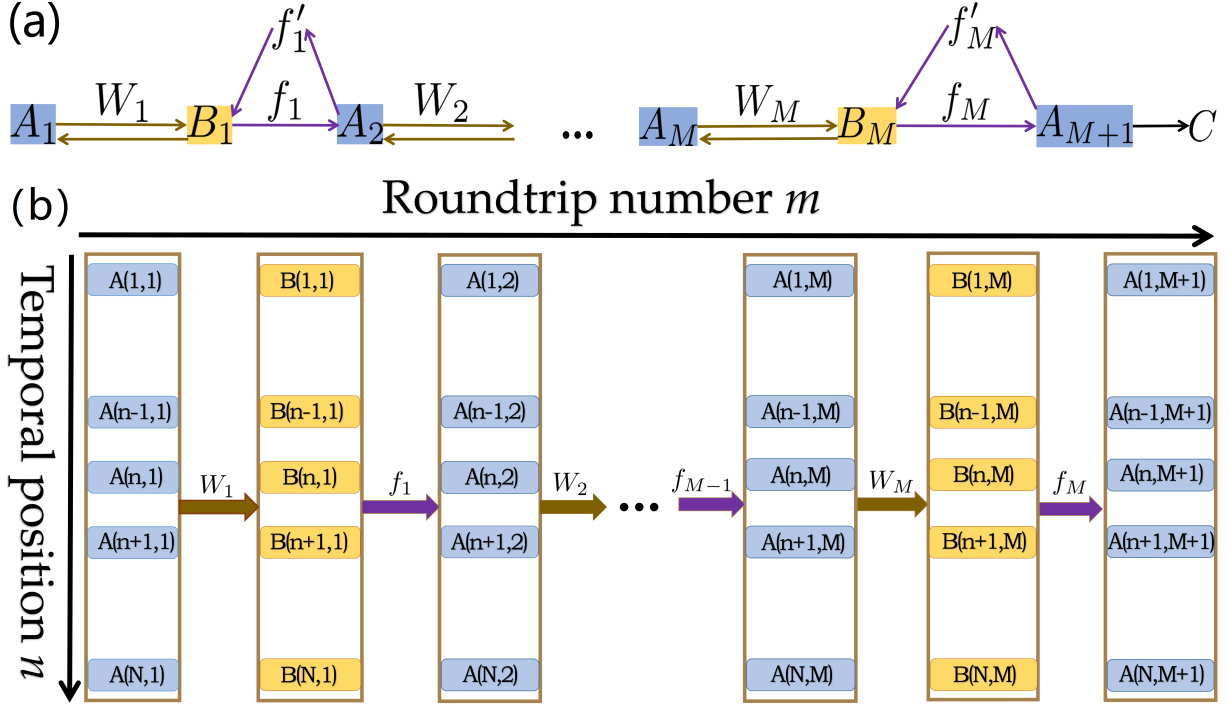


FIG. 3: (a) Schematic of the architecture of an optical neural network. A_1 is the vector of pulses imported in the first layer when training starts. A_m : vector of the output pulses after the $m - 1$ -th roundtrip (layer), which is also the input vector for the m -th roundtrip (layer); W_m : matrix for the linear transformation during the m -th roundtrip (layer); B_m : vector of pulses after the linear transformation during the m -th roundtrip (layer); f_m : nonlinear activation operation; f'_m : derivative of f_m during back propagation. C is the cost function for the output signal. (b) Illustration of the signal flow through roundtrips (layers) in the resonator in Fig. 2(a).

$$A_{m+1} = f_m B_m, \quad (5)$$

where A_m and B_m are vectors of $A(n, m)$ and $B(n, m)$, respectively. Pulse information $A(n, m + 1)$ ($B(n, m)$) after (before) the nonlinear operation at the n -th temporal position during the m -th roundtrip can be collected by dropping a very small portion of pulses out of the resonator network into detectors. Such information of A_m and B_m is stored in the computer for further backward propagation in training the ONN.

Once the forward propagation is finished after M roundtrips in the optical resonator network, the backward propagation can be performed in the computer following the standard

procedure [17, 54]:

$$\tilde{B}_m = B_m + f'_m(A_{m+1} - \tilde{A}_{m+1}), \quad (6)$$

$$\tilde{A}_m = W_m^T \tilde{B}_m, \quad (7)$$

\tilde{A}_m and \tilde{B}_m are vectors at the m -th layer, calculated through the back propagation from the stored information of A_{m+1} and B_m . Here f'_m is the derivative of the nonlinear operation at the m -th layer in Eq. (5), W_m^T is the transpose of W_m in Eq. (4), and \tilde{A}_{M+1} is the target vector A_{target} , which is the expected output vector of the training set. The cost function after the m -th layer can therefore be calculated as:

$$C_m = \frac{1}{2N} \sum_{i=1}^N |A(i, m+1) - \tilde{A}(i, m+1)|^2. \quad (8)$$

Throughout the backward propagation, optical controlling parameters $\phi_1(n, m)$, $\phi_2(n, m)$, $\theta_1(n, m)$, $\theta_2(n, m)$, and $\theta_3(n, m)$ can be trained by calculating the derivative of C_m with respect to these parameters, i.e.,

$$\frac{\partial C_m}{\partial \phi_{1,2}(n, m)} = [(A_{m+1} - \tilde{A}_{m+1})]^T \odot f'_m \cdot \frac{\partial W^T}{\partial \phi_{1,2}(n, m)} \cdot A_m, \quad (9)$$

$$\frac{\partial C_m}{\partial \theta_{1,2,3}(n, m)} = [(A_{m+1} - \tilde{A}_{m+1})]^T \odot f'_m \cdot \frac{\partial W^T}{\partial \theta_{1,2,3}(n, m)} \cdot A_m, \quad (10)$$

\odot is the vector multiplication, with $\mathbf{c} = \mathbf{a} \odot \mathbf{b}$ defined as $c_n = a_n b_n$. We can obtain the corrections of parameters as [54]:

$$\Delta \phi_{1,2}(n, m) = -a \frac{\partial C_m}{\partial \phi_{1,2}(n, m)}, \quad (11)$$

$$\Delta \theta_{1,2,3}(n, m) = -a \frac{\partial C_m}{\partial \theta_{1,2,3}(n, m)}, \quad (12)$$

where a is learning rate for this training. Then $\phi_{1,2}(n, m)$ becomes $\phi_{1,2}(n, m) + \Delta \phi_{1,2}(n, m)$ and $\theta_{1,2,3}(n, m)$ becomes $\theta_{1,2,3}(n, m) + \Delta \theta_{1,2,3}(n, m)$. Following the backward propagation procedure summarized above, the parameters for controlling the forward propagation of each pulse at the n -th temporal position for the m -th roundtrip are updated backwardly from the M -th layer to the 1st layer.

At this point, we discuss a training iteration which is composed of the forward propagation by optical pulses and the backward propagation by the computer algorithm. To prepare the ONN ready for the proper computation, one needs to repeat training iterations for an enough

iteration number. Once the training procedure is finished after a certain number of iterations, all controlling parameters in the resonator network are finalized, and the ONN with the temporal synthetic dimension is ready for doing the designed all-optical computation with optical pulses in this single resonator network.

III. RESULTS

As an illustration, we choose the wine classification problem to train our proposed ONN with training sets of data and test the computation accuracy of the ONN with test sets of data from Ref. [51]. A wine classification problem is a well-established example to test the validity of an artificial neural network. This problem uses the input information that one can directly measure from the wine such as yeast content, sugar content, and preservation time and computes the output information that one can not obtain directly from the wine including the quality of soil in which grapes grow, annual precipitation of the vineyard, and the degree to which grapes are planted sparsely. The hidden relationship between the known information and the desired information can be captured by the artificial neural network after one trains it [51]. Here, we use the proposed ONN with the temporal synthetic dimension to conduct this specific problem. The input set of optical pulses with prepared complex amplitudes carry arrays of data from the input information, while the output pulses from the proposed ONN give the arrays of data after the computation.

In simulations, we choose 178 pulses in one roundtrip (i.e., $N=178$) and $M=10$, a total number of 10 roundtrips, for training this specific problem with our proposed the ONN. 80,000 sets of training data are used. Moreover, $a=0.003$ is taken. After each iteration of training, we conduct the computation with the test sets to measure how accurate our ONN becomes. In Figs. 4(a) and 4(b), we plot the normalized cost functions for training sets and test sets versus the computation iteration number, respectively. One can see both cost functions are gradually decreasing when we perform more iterated training procedure. To see the accuracy of the trained ONN, we define P to compare the similarities between the output vector computed from ONN and the expected vector [55]:

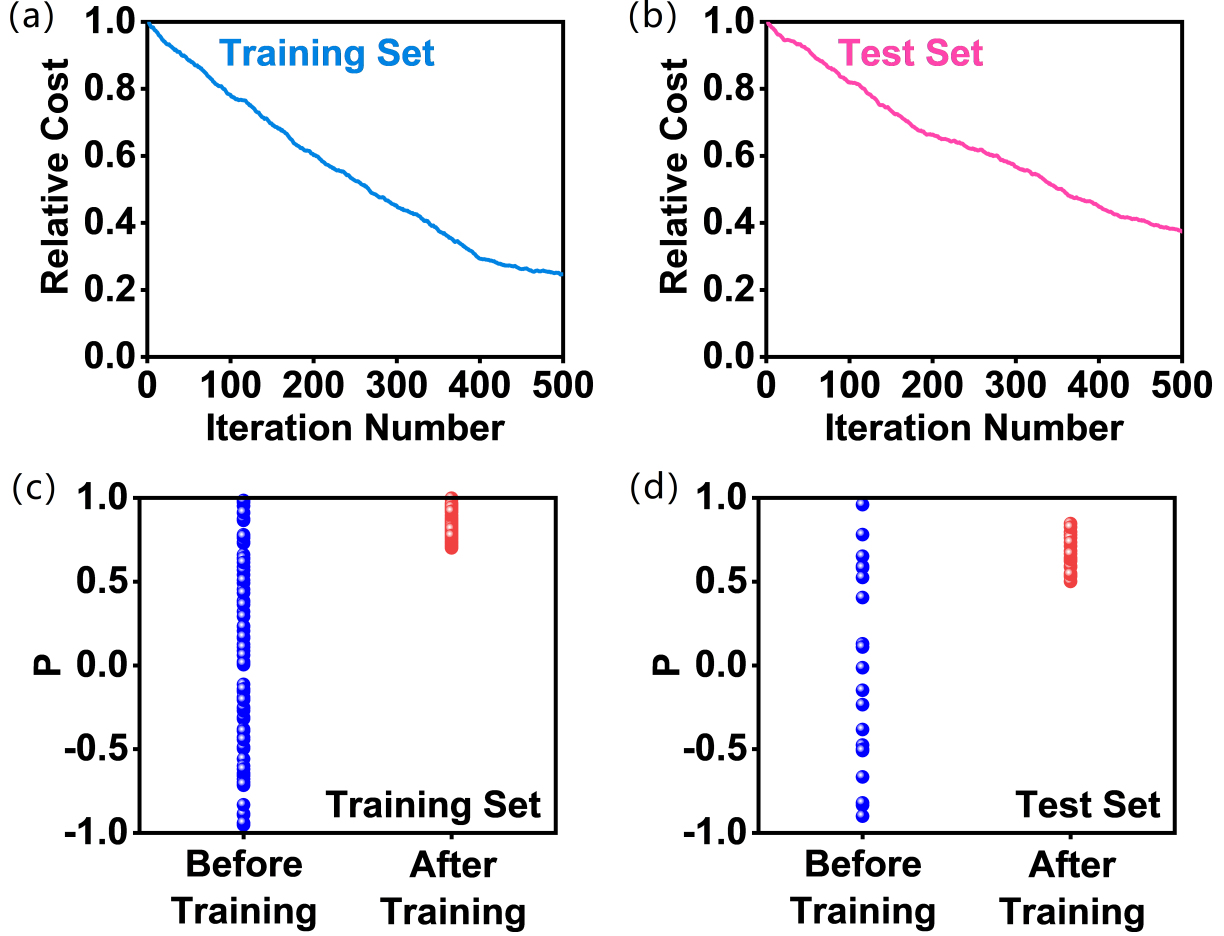


FIG. 4: (a)–(b) Relative cost functions defined as Eq. (8) versus the training iteration number during the training process for (a) training sets and (b) test sets, respectively. (c)–(d) Representative P -values that denotes the computation accuracy (defined in Eq. (13)) before and after training with the iteration number being 500 for (c) training sets and (d) test sets, respectively.

$$P = \frac{\text{Re} \left[\sum_{i=1}^N A(i, M + 1) A(i, \text{target}) \right]}{\sqrt{\sum_{i=1}^N |A(i, M + 1)|^2} \sqrt{\sum_{i=1}^N |A(i, \text{target})|^2}}. \quad (13)$$

Here, $A(i, \text{target})$ gives the set of real numbers of the expected vector and P is the cosine of the angles between the output vectors and expected vectors. Therefore P denotes the agreement between two vectors, where $P = 1$ labels the exact matching between two vectors and $P = 0$ means that two vectors are orthogonal. We plot P computed from ONN before the training and after the training with the training sets and test sets of data in Figs. 4(c) and 4(d), respectively. Before the training, P from both the training sets and test sets

spread randomly at the range from -1 to 1 , meaning that the ONN does not make a good connection between the known information and the desired information. Nevertheless, after the training, P from the training sets is close to unity with significantly decreased variation, and P from the testing sets is also distributed in the range from 0.5 to 1 , meaning that the ONN after training can perform desired computation with reasonably good accuracy.

Our chosen example of the wine classification is a relatively complex computation problem, yet the training from the ONN with the synthetic temporal dimension still works well. The number of optical pulses determines the capacity for carrying information while the number of roundtrips provides the total layer numbers in the ONN. Therefore, it is flexible to choose different numbers of pulses and roundtrips dependent on different specific problems and how accuracy of the ONN is desired. We therefore outlook our proposed ONN can be an alternative platform to conduct all-optical computations with different desired targets after the training.

The proposed platform is experimentally feasible with the state-of-the-art photonic technology. The fiber ring resonator with kilometer-long roundtrip length can be constructed with hundreds of temporal separated pulses circulating inside the resonator [40]. The nonlinear saturable absorber has been demonstrated with graphene layers [53, 56]. Such platform for achieving the temporal synthetic dimension can also be realized in a resonator with the free-space optics [42]. In both setups, delay lines (channels) are used to create the nearest-neighbor couplings along the temporal synthetic dimension. Moreover, appropriate delay lines (channels) can also connect pulses at time separations with double, triple, and/or high-order Δt , i.e., providing the long-range couplings. It therefore holds the possibility for generating more than three connectivities between sites in two layers in Fig. 2(b), which might be possible to further increase the accuracy of the ONN.

IV. CONCLUSION

In summary, we propose a novel method to create the ONN in a single resonator network with the concept of the temporal synthetic dimension. Two delay lines have been used to connect temporal-nearby pulses in each roundtrip, with the detailed dynamics being controlled by parameters in splitters and phase modulators. By including the nonlinear saturable absorber, pulses in each roundtrip become one layer in the ONN, and forward

transmission with linear transformation and nonlinear operation is conducted when pulses circulate inside the resonator after each roundtrip. Backward propagation is done by the computer to train all control parameters. As the proof of principle, we show the complicated wine classification problem in numerical simulations, which works quite well. Our proposed ONN in the temporal synthetic dimension is flexible, which can be re-configurable and scalable on the number of sites (pulses) in each layers as well as the number of layers (roundtrips) for each computation. Once getting trained, the ONN operates all-optically. Furthermore, one can also prepare the set of pulses with the single-photon state instead [42], which might makes our proposal with the temporal synthetic dimension being possible for constructing the quantum neural network in the future study. Our work therefore shows the opportunity for constructing a flexible ONN in a single resonator, which points to a broad range of potential applications from all-optical computation to optical information processing in both benchtop optics and on-chip photonics.

Acknowledgments

The research is supported by National Natural Science Foundation of China (11974245), National Key R&D Program of China (2017YFA0303701), Shanghai Municipal Science and Technology Major Project (2019SHZDZX01), and Natural Science Foundation of Shanghai (19ZR1475700). V. V. Y. acknowledges partial funding from NSF (DBI-1455671, ECCS-1509268, CMMI-1826078), AFOSR (FA9550-15-1-0517, FA9550-18-1-0141, FA9550-20-1-0366, FA9550-20-1-0367), DOD Army Medical Research (W81XWH2010777), NIH (1R01GM127696-01, 1R21GM142107-01), and the Cancer Prevention and Research Institute of Texas (RP180588). L. Y. acknowledges support from the Program for Professor of Special Appointment (Eastern Scholar) at Shanghai Institutions of Higher Learning. X. C. also acknowledges the support from Shandong Quancheng Scholarship (00242019024).

-
- [1] D. Rosenbluth, K. Kravtsov, M. P. Fok, and P. R. Prucnal, “A high performance photonic pulse processing device,” *Optics Express* **17**, 22767-22772 (2009).
 - [2] A. N. Tait, M. A. Nahmias, B. J. Shastri, and P. R. Prucnal, “Broadcast and weight: an integrated network for scalable photonic spike processing,” *Journal of Lightwave Technology*

- 32**, 4029-4041 (2014).
- [3] Y. Shen, N. C. Harris, S. Skirlo, M. Prabhu, T. Baehr-Jones, M. Hochberg, X. Sun, S. Zhao, H. Larochelle, D. Englund, and M. Soljačić, “Deep learning with coherent nanophotonic circuits,” *Nature Photonics* **11**, 441-446 (2017).
- [4] A. N. Tait, T. F. de Lima, E. Zhou, A. X. Wu, M. A. Nahmias, B. J. Shastri, and P. R. Prucnal, “Neuromorphic photonic networks using silicon photonic weight banks,” *Scientific Reports* **7**, 7430 (2017).
- [5] X. Lin, Y. Rivenson, N. T. Yardimci, M. Veli, Y. Luo, M. Jarrahi, and A. Ozcan, “All-optical machine learning using diffractive deep neural networks,” *Science* **361**, 1004-1008 (2018).
- [6] Z. Ying, Z. Wang, Z. Zhao, S. Dhar, D. Z. Pan, R. Soref, and R. T. Chen, “Silicon microdisk-based full adders for optical computing,” *Optics Letters* **43**, 983-986 (2018).
- [7] J. Feldmann, N. Youngblood, C. D. Wright, H. Bhaskaran, and W. H. P. Pernice, “All-optical spiking neurosynaptic networks with self-learning capabilities,” *Nature* **569**, 208-214 (2019).
- [8] Y. Zuo, B. Li, Y. Zhao, Y. Jiang, Y.-C. Chen, P. Chen, G.-B. Jo, J. Liu, and S. Du, “All-optical neural network with nonlinear activation functions,” *Optica* **6**, 1132-1137 (2019).
- [9] R. Hamerly, L. Bernstein, A. Sludds, M. Soljačić, and D. Englund, “Large-scale optical neural networks based on photoelectric multiplication,” *Physical Review X* **9**, 021032 (2019).
- [10] E. Khoram, A. Chen, D. Liu, L. Ying, Q. Wang, M. Yuan, and Z. Yu, “Nanophotonic media for artificial neural inference,” *Photonics Research* **7**, 823-827 (2019).
- [11] G. Wetzstein, A. Ozcan, S. Gigan, S. Fan, D. Englund, M. Soljačić, C. Denz, D. A. B. Miller, and D. Psaltis, “Inference in artificial intelligence with deep optics and photonics,” *Nature* **588**, 39-47 (2020).
- [12] M. A. Nahmias, T. F. de Lima, A. N. Tait, H.-T. Peng, B. J. Shastri, and P. R. Prucnal, “Photonic multiply-accumulate operations for neural networks,” *IEEE Journal of Selected Topics in Quantum Electronics* **26**, 1-18 (2020).
- [13] W. Bogaerts, D. Pérez, J. Capmany, D. A. B. Miller, J. Poon, D. Englund, F. Morichetti, and A. Melloni, “Programmable photonic circuits,” *Nature* **586**, 207-216 (2020).
- [14] X. Xu, M. Tan, B. Corcoran, J. Wu, A. Boes, T. G. Nguyen, S. T. Chu, B. E. Little, D. G. Hicks, R. Morandotti, A. Mitchell, and D. J. Moss, “11 TOPS photonic convolutional accelerator for optical neural networks,” *Nature* **589**, 44-51 (2021).
- [15] J. Feldmann, N. Youngblood, M. Karpov, H. Gehring, X. Li, M. Stappers, M. Le Gallo, X.

- Fu, A. Lukashchuk, A. S. Raja, J. Liu, C. D. Wright, A. Sebastian, T. J. Kippenberg, W. H. P. Pernice, and H. Bhaskaran, “Parallel convolutional processing using an integrated photonic tensor core,” *Nature* **589**, 52-58 (2021).
- [16] J. Jiang, M. Chen, and J. A. Fan, “Deep neural networks for the evaluation and design of photonic devices,” *Nature Reviews Materials* (2020). <https://doi.org/10.1038/s41578-020-00260-1>
- [17] T. W. Hughes, M. Minkov, Y. Shi, and S. Fan, “Training of photonic neural networks through in situ back-propagation and gradient measurement,” *Optica* **5**, 864-871 (2018).
- [18] T. Zhou, L. Fang, T. Yan, J. Wu, Y. Li, J. Fan, H. Wu, X. Lin, and Q. Dai “In situ optical backpropagation training of diffractive optical neural networks,” *Photonics Research* **8**, 940-953 (2020).
- [19] G. R. Steinbrecher, J. P. Olson, D. Englund, and J. Carolan, “Quantum optical neural networks,” *npj Quantum Information* **5**, 60 (2019).
- [20] L. Yuan, Q. Lin, M. Xiao, and S. Fan, “Synthetic dimension in photonics,” *Optica* **5**, 1396-1405 (2018).
- [21] T. Ozawa, and H. M. Price, “Topological quantum matter in synthetic dimensions,” *Nature Reviews Physics* **1**, 349-357 (2019).
- [22] T. Ozawa, H. M. Price, N. Goldman, O. Zilberberg, and I. Carusotto, “Synthetic dimensions in integrated photonics: from optical isolation to four-dimensional quantum Hall physics,” *Physical Review A* **93**, 043827 (2016).
- [23] L. J. Maczewsky, K. Wang, A. A. Dovgiy, A. E. Miroshnichenko, A. Moroz, M. Ehrhardt, M. Heinrich, D. N. Christodoulides, A. Szameit, and A. A. Sukhorukov, “Synthesizing multi-dimensional excitation dynamics and localization transition in one-dimensional lattices,” *Nature Photonics* **14**, 76-81 (2020).
- [24] A. Schwartz and B. Fischer, “Laser mode hyper-combs,” *Optics Express* **21**, 6196-6204 (2013).
- [25] D. Jukić, and H. Buljan, “Four-dimensional photonic lattices and discrete tesseract solitons,” *Physical Review A* **87**, 013814 (2013).
- [26] L. Yuan, M. Xiao, Q. Lin, and S. Fan, “Synthetic space with arbitrary dimensions in a few rings undergoing dynamic modulation,” *Physical Review B* **97**, 104105 (2018).
- [27] E. Lustig, S. Weimann, Y. Plotnik, Y. Lumer, M. A. Bandres, A. Szameit, and M. Segev, “Photonic topological insulator in synthetic dimensions,” *Nature* **567**, 356-360 (2019).

- [28] A. Dutt, Q. Lin, L. Yuan, M. Minkov, M. Xiao, and S. Fan, “A single photonic cavity with two independent physical synthetic dimensions,” *Science* **367**, 59-64 (2020).
- [29] D. Yu, L. Yuan, and X. Chen. “Isolated photonic flatband with the effective magnetic flux in a synthetic space including the frequency dimension,” *Laser & Photonics Reviews* **14**, 2000014 (2020).
- [30] L. Yuan, A. Dutt, M. Qin, S. Fan, and X. Chen, “Creating locally interacting Hamiltonians in the synthetic frequency dimension for photons,” *Photonics Research* **8**, B8-B14 (2020).
- [31] G. Li, Y. Zheng, A. Dutt, D. Yu, Q. Shan, S. Liu, L. Yuan, S. Fan, and X. Chen “Dynamic band structure measurement in the synthetic space,” *Science Advances* **7**, eabe4335 (2021).
- [32] L. Yuan, Y. Shi, and S. Fan, “Photonic gauge potential in a system with a synthetic frequency dimension,” *Optics Letters* **41**, 741-744 (2016).
- [33] B. A. Bell, K. Wang, A. S. Solntsev, D. N. Neshev, A. A. Sukhorukov, and B. J. Eggleton, “Spectral photonic lattices with complex long-range coupling,” *Optica* **4**, 1433-1346 (2017).
- [34] C. Qin, F. Zhou, Y. Peng, D. Sounas, X. Zhu, B. Wang, J. Dong, X. Zhang, A. Alú, and P. Lu, “Spectrum control through discrete frequency diffraction in the presence of photonic gauge potentials,” *Physical Review Letters* **120**, 133901 (2018).
- [35] A. Dutt, M. Minkov, Q. Lin, L. Yuan, D. A. B. Miller, and S. Fan, “Experimental band structure spectroscopy along a synthetic dimension,” *Nature Communications* **10**, 3122 (2019).
- [36] X.-W. Luo, X. Zhou, C.-F. Li, J.-S. Xu, G.-C. Guo and Z.-W. Zhou, “Quantum simulation of 2D topological physics in a 1D array of optical cavities,” *Nature Communications* **6**, 7044 (2015).
- [37] A. Regensburger, C. Bersch, B. Hinrichs, G. Onishchukov, A. Schreiber, C. Silberhorn, and U. Peschel, “Photon propagation in a discrete fiber network: an interplay of coherence and losses,” *Physical Review Letters* **107**, 233902 (2011).
- [38] A. Regensburger, C. Bersch, M.-A. Miri, G. Onishchukov, D. N. Christodoulides, and U. Peschel, “Parity-time synthetic photonic lattices,” *Nature* **488**, 167-171 (2012).
- [39] M. Wimmer, A. Regensburger, C. Bersch, M.-A. Miri, S. Batz, G. Onishchukov, D. N. Christodoulides, and U. Peschel, “Optical diametric drive acceleration through action-reaction symmetry breaking,” *Nature Physics* **9**, 780-784 (2013).
- [40] A. Marandi, Z. Wang, K. Takata, R. L. Byer, and Y. Yamamoto, “Network of time-multiplexed optical parametric oscillators as a coherent Ising machining,” *Nature Photonics* **8**, 937-942

- (2014).
- [41] M. Wimmer, H. M. Price, I. Carusotto, and U. Peschel, “Experimental measurement of the Berry curvature from anomalous transport,” *Nature Physics* **13**, 545-550 (2017).
 - [42] C. Chen, X. Ding, J. Qin, Y. He, Y.-H. Luo, M.-C. Chen, C. Liu, X.-L. Wang, W.-J. Zhang, H. Li, L.-X. You, Z. Wang, D.-W. Wang, B. C. Sanders, C.-Y. Lu, and J.-W. Pan, “Observation of topologically protected edge states in a photonic two-dimensional quantum walk,” *Physical Review Letters* **121**, 100502 (2018).
 - [43] T. Ozawa, H. M. Price, A. Amo, N. Goldman, M. Hafezi, L. Lu, M. C. Rechtsman, D. Schuster, J. Simon, O. Zilberberg, and I. Carusotto, “Topological photonics,” *Reviews of Modern Physics* **91**, 015006 (2019).
 - [44] M. Segev and M. A. Bandres, “Topological photonics: where do we go from here?” *Nanophotonics* **10**, 425-434 (2020).
 - [45] L. Huang, L. Xu, M. Woolley, and A. E. Miroshnichenko, “Trends in quantum nanophotonics,” *Advanced Quantum Technologies* **3**, 1900126 (2020).
 - [46] D. Leykam and L. Yuan, “Topological phases in ring resonators: recent progress and future prospects,” *Nanophotonics* **9**, 4473-4487 (2020).
 - [47] A. V. Pankov, O. S. Sidelnikov, I. D. Vatnik, A. A. Sukhorukov, and D. V. Churkin, “Deep learning with synthetic photonic lattices for equalization in optical transmission systems,” *Proc. SPIE 11192, Real-time Photonics Measurements, Data Management, and Processing IV*, 111920N (2019).
 - [48] S. Buddhiraju, A. Dutt, M. Minkov, I. A. D. Williamson, and S. Fan, “Arbitrary linear transformations for photons in the frequency synthetic dimension,” arXiv:2009.02008 (2020).
 - [49] Z. Lin, S. Sun, J. Azana, W. Li, N. Zhu, and M. Li, “Temporal optical neurons for serial deep learning,” arXiv:2009.03213 (2020).
 - [50] H. Chalabi, S. Barik, S. Mittal, T. E. Murphy, M. Hafezi, and E. Waks, “Synthetic gauge field for two-dimensional time-multiplexed quantum random walks,” *Physical Review Letters* **123**, 150503 (2019).
 - [51] J. Alcalá-Fdez, A. Fernández, J. Luengo, J. Derrac, S. García, L. Sánchez, and F. Herrera, “KEEL data-mining software tool: data set repository, integration of algorithms and experimental analysis framework,” *Journal of Multiple-Valued Logic and Soft Computing* **17**, 255-287 (2011).

- [52] Y. LeCun, Y. Bengio, and G. Hinton, “Deep learning,” *Nature* **521**, 436-444 (2015).
- [53] Q. Bao, H. Zhang, Z. Ni, Y. Wang, L. Polavarapu, Z. Shen, Q.-H Xu, D. Tang, and K. P. Loh, “Monolayer graphene as a saturable absorber in a mode-locked laser,” *Nano Research* **4**, 297-307 (2011).
- [54] Y. Bengio, “Learning deep architectures for AI,” *Foundations and Trends in Machine Learning* **2**, 1-127 (2009).
- [55] P.-N. Tan, M. Steinbach, and V. Kumar, “Introduction to Data Mining,” Pearson Education (2006).
- [56] Z. Cheng, H. K. Tsang, X. Wang, K. Xu, and J.-B. Xu, “In-plane optical absorption and free carrier absorption in graphene-on-silicon waveguides,” *IEEE Journal of Selected Topics in Quantum Electronics* **20**, 43-48 (2014).